Computational Screening of Phthalate Monoesters for Binding to PPARγ

Taner Kaya,[†,‡] Scott C. Mohr,[†] David J. Waxman,[§] and Sandor Vajda*[,‡]

Departments of Chemistry, Biomedical Engineering, and Biology, Boston University, Boston, Massachusetts 02215

Received October 27, 2005

Phthalate esters are ubiquitous environmental contaminants that interact with peroxisome proliferator-activated receptors (PPARs), a family of nuclear receptors. Molecular docking and free energy calculations were performed in an effort to identify novel phthalate ligands of PPARγ, a subtype expressed in a wide range of human tissues. The method was validated using several agonists and partial agonists of PPARγ, whose binding orientations were correctly reproduced; however, reduced accuracy in docking was observed with ligands of increasing size and flexibility. Improved results were obtained by introduction of a more accurate scoring function based on the all-atom molecular mechanics potential CHARMM and a generalized born/surface area solvation term ACE (analytical continuum electrostatics). Comparison of the lowest CHARMM/ACE energy of each phthalate vs the logarithm of the experimentally determined that EC_{50} values for PPARγ trans-activation yielded a good correlation ($R^2 = 0.82$). Thus, we can reliably distinguish phthalates that bind and activate PPARγ from those that do not, with the computational method predicting relative PPARγ binding activities with some degree of accuracy. We have applied this method to screen a series of 73 mono-*ortho*-phthalate esters listed in the Available Chemicals Directory. Several putative PPARγ binding phthalates were identified, including compounds that are known PPARγ agonists. These findings support the use of computational methods to identify environmental chemicals that warrant further experimental evaluation for PPAR binding and trans-activation potential in cell-based models.

Introduction

Phthalate esters are widely used as plasticizers in the manufacture of products made of poly(vinyl chloride) and other plastics (*1*). Di-(2-ethylhexyl) phthalate (DEHP), for example, is added in varying amounts to certain plastics to increase their flexibility. The plasticizers readily leach from plastic surfaces, and thus, phthalates are major environmental contaminants in water, food, and soil, resulting in extensive human exposure (*2*, *3*). The pathological consequences of human exposure to environmental levels of DEHP are uncertain (*4*). However, it is metabolized to mono-(2-ethylhexyl) phthalate (MEHP), a known hepatocarcinogen (*5*) and gonadal toxicant in rodents (*6*).

The carcinogenicity of MEHP is in part linked to its activation of the peroxisome proliferator-activated receptor α (PPARα), a ligand-activated transcription factor belonging to the nuclear receptor family. Recent work has demonstrated that MEHP can also activate mouse and human PPARγ (*7*), which is highly expressed in human adipose tissue where many lipophilic foreign chemicals tend to accumulate, as well as in colon, heart, liver, testis, spleen, and hematopoietic cells. Substantial human urinary levels of several other phthalate monoesters, notably monobenzyl phthalate and monobutyl phthalate, have been reported (*2*, *3*) raising the question of whether significant PPAR activation, and perhaps adverse health effects, accompany environmental or occupational exposure to these chemicals as well. Support for this possibility comes from a recent, and at this point unconfirmed, report by Swan et al. (*8*), which indicates the likelihood that observed abnormalities in human male infant reproductive development stem from prenatal exposure to a mixture of phthalate metabolites.

Two recent studies focused on the activation of PPARs by phthalate monoesters. Hurst and Waxman (*7*) assayed phthalate activation of PPARγ, as well as the activation of PPARα, in transfected COS cells and in a PPARγ-responsive adipocyte cell line. Monobenzyl phthalate was found to activate both mouse and human PPARγ, with effective concentrations for half-maximal response (EC_{50}) values between 75 and 100 μM. MEHP was ~10-fold more potent as an activator of PPARγ, with EC_{50} values between 6.2 and 10.1 μM. No significant PPAR activation was observed with the monomethyl, mono-*n*-butyl, dimethyl, or diethyl esters of phthalic acid.

Lampen et al. (*9*) tested the activity of two diphthalate esters and 19 monophthalate esters using two in vitro test systems: cell differentiation in F9 teratocarcinoma and activation of PPAR ligand binding domain (LBD) in Chinese hamster ovary reporter cells. All three PPAR subtypes (α, β/δ, and γ) were included in the analysis. Five of the compounds, MEHP, mono-(1-methylheptyl) phthalate, monobenzyl phthalate, butylbenzyl phthalate, and 2-ethylhexanoic acid, induced F9 cell differentiation. The other test compounds failed to induce differentiation of these cells. Four compounds [monomethyl phthalate, monoethyl phthalate, mono-(2,2-dimethyl-1-phenylpropyl) phthalate, and dimethyl phthalate] did not interact with any PPARs. All other phthalate esters activated PPARγ, in some cases more strongly than they activated PPARα, with EC_{50} values ranging from 15 to 750 μM.

In the present paper, we tested the hypothesis that computational docking methods could successfully screen for phtha-

* To whom correspondence should be addressed. Tel: 617-353-4757. Fax: 617-353-6766. E-mail: vajda@bu.edu.
[†] Department of Chemistry.
[‡] Department of Biomedical Engineering.
[§] Department of Biology.

10.1021/tx050301s CCC: $33.50
Published on Web 00/00/0000 PAGE EST: 11

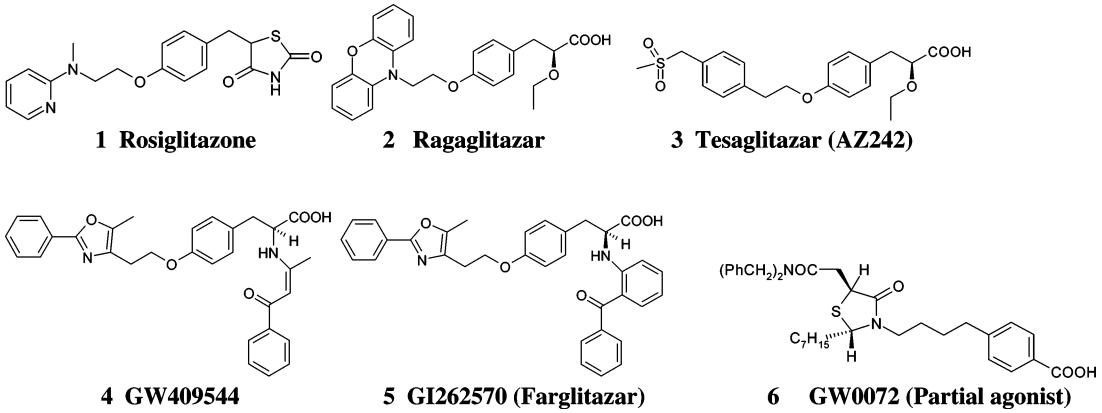

Figure 1. Structures of the PPAR-γ agonists used in this work.

lates likely to interact with PPARγ. Our primary tool was the docking program GOLD (Genetic Optimization for Ligand Docking) (*10*, *11*), one of the best docking programs currently available (*12*, *13*). Because all docking methods have somewhat limited accuracy and reliability (*14*) and PPARγ has a large and deep binding site (*15*), which makes docking particularly difficult, we have performed extensive validation tests using binding data on PPARγ ligands and a number of phthalates. The results of these tests suggested that we can reliably distinguish PPARγ binding phthalates from those that do not bind. Therefore, we proceeded to dock each of the 73 *ortho*-phthalate esters included in the Available Chemicals Directory (ACD) and identified several phthalates that are as likely to interact with PPARγ as some of the known activators. Our results suggest that the computational method represents a relatively inexpensive first step in screening for environmental chemicals interacting with a particular protein.

Materials and Methods

Outline of Validation Procedures. Two validation tests were performed as follows. (i) We took six PPARγ structures available in the Proten Data Bank or PDB (*16*) that were cocrystallized with different agonists, removed the ligands computationally, and then rebuilt the complexes from their component molecules using GOLD. This enabled us to ascertain whether near-native conformations could be obtained and whether the scoring function can discriminate acceptable structures from ones that are far from the native structure. By refining and rescoring the docked conformations using the molecular mechanics potential function CHARMM (*17*, *18*) with the analytical continuum electrostatic (ACE) electrostatic and solvation model (*19*), we obtained better results than with GOLD alone. The ensemble of structures generated also provided information on the variability of the docked structures. (ii) In the second validation step, we applied the docking methodology to the 16 phthalate monoesters experimentally studied by Lampen et al. (*9*).

Molecular Structures. In the first validation step, we docked six known agonists of PPARγ (Figure 1) to PPARγ structures from the PDB (*16*). Each structure is identified by its four-character PDB code and the specific chain studied. The selected chains are as follows: 2prg chain A, with the PPARγ agonist rosiglitazone (*14*); 1nyx chain A, with the agonist ragaglitazar (*20*, *21*); 1i71 chain A, with the agonist tesaglitazar (also known as AZ242) (*22*); 1k74 chain D, with the agonist GW409544 (*23*); 1fm9 chain D, with agonist GI262570 (also known as farglitazar) (*24*); and 4prg chain A, with the partial agonist GW0072 (*25*). Because the short C-terminal α-helix (H12) of PPARγ—also referred to as the ligand-dependent activating function domain (AF-2 domain)—plays a critical role in the activation of PPAR transcriptional activity (*26*, *27*), in the case of homo- or heterodimeric PPARγ structures (*19*), we selected the chain that had helix H12 in a more closed, activelike conformation (*28*, *29*). Prior to docking, water molecules and all ligands were removed. We used the MOE program (Chemical Computing Group, Toronto, Canada) for adding hydrogen atoms, for assigning Gasteiger partial charges (*30*) to all protein atoms, and for performing a short minimization to refine hydrogen positions in the complex.

All ligand molecules were docked starting from their "standard" structures, which were obtained from the ACD or were built using MOE. For screening calculations, the SMILES filtering option of the VIDA software (OpenEye Scientific Software, Santa Fe, NM) was used to select the mono-*ortho*-phthalates from the ACD. Hydrogen atoms and partial charges were added to the ligands using the BABEL package (*31*).

Docking. All docking runs were performed using GOLD, a genetic algorithm-based program for calculating the docking modes of small molecules at protein binding sites (*10*, *11*). GOLD was used with its default settings. The search during the docking allowed for full ligand and partial protein flexibility, the latter being restricted to torsional degrees of freedom in side chains with hydrogen-bonding capability. For each ligand, docking was performed for 50 separate runs, and results were clustered on the basis of pairwise root mean square deviation (RMSD) calculations. In each run, solutions were evaluated by the energy function

$$\Delta G_{\mathrm{GOLD}} = \Delta E_{\mathrm{ext-VDW}} + \Delta E_{\mathrm{ext-H}} + \Delta E_{\mathrm{int-tor}} + \Delta E_{\mathrm{int-VDW}}$$

where $\Delta E_{\mathrm{ext-VDW}}$ and $\Delta E_{\mathrm{ext-H}}$ denote the external van der Waals (VDW) and the hydrogen-bonding energy terms, respectively, between the protein and the ligand; $\Delta E_{\mathrm{int-tor}}$ is the torsional strain energy of the ligand; and $\Delta E_{\mathrm{int-VDW}}$ is the internal VDW energy of the ligand. The quantity referred to as the GOLD score is $-\Delta G_{\mathrm{GOLD}}$.

Scoring by the CHARMM/ACE Potential. The fittest solution generated in each of the 50 GOLD docking runs was refined by performing 100 energy minimization steps using the CHARMM/ACE potential (*17*−*19*) of the form

$$\mathrm{E}_{\mathrm{CHARMM}} = E_{\mathrm{VDW}} + E_{\mathrm{int}} + E_{\mathrm{elec}} + G_{\mathrm{des}}$$

where E_{VDW}, E_{elec}, and G_{des} denote the VDW, electrostatic, and desolvation energy terms, respectively. The VDW term is calculated by the Lennard−Jones 6−12 potential (*16*), and the sum $E_{\mathrm{elec}} + G_{\mathrm{des}}$ is based on the ACE model (*18*). The internal (bonded) energy, E_{int}, is the sum of bond stretching, angle bending, torsional, and improper terms:

$$E_{\mathrm{int}} = E_{\mathrm{bond}} + E_{\mathrm{angle}} + E_{\mathrm{dihed}} + E_{\mathrm{improper}}$$

calculated by the CHARMM potential. The binding free energy, ΔG, is calculated using these bound and unbound E_{CHARMM} values:

$$\Delta G_{\mathrm{CHARMM}} = E_{\mathrm{complex}} - E_{\mathrm{ligand}} - E_{\mathrm{prot}}$$

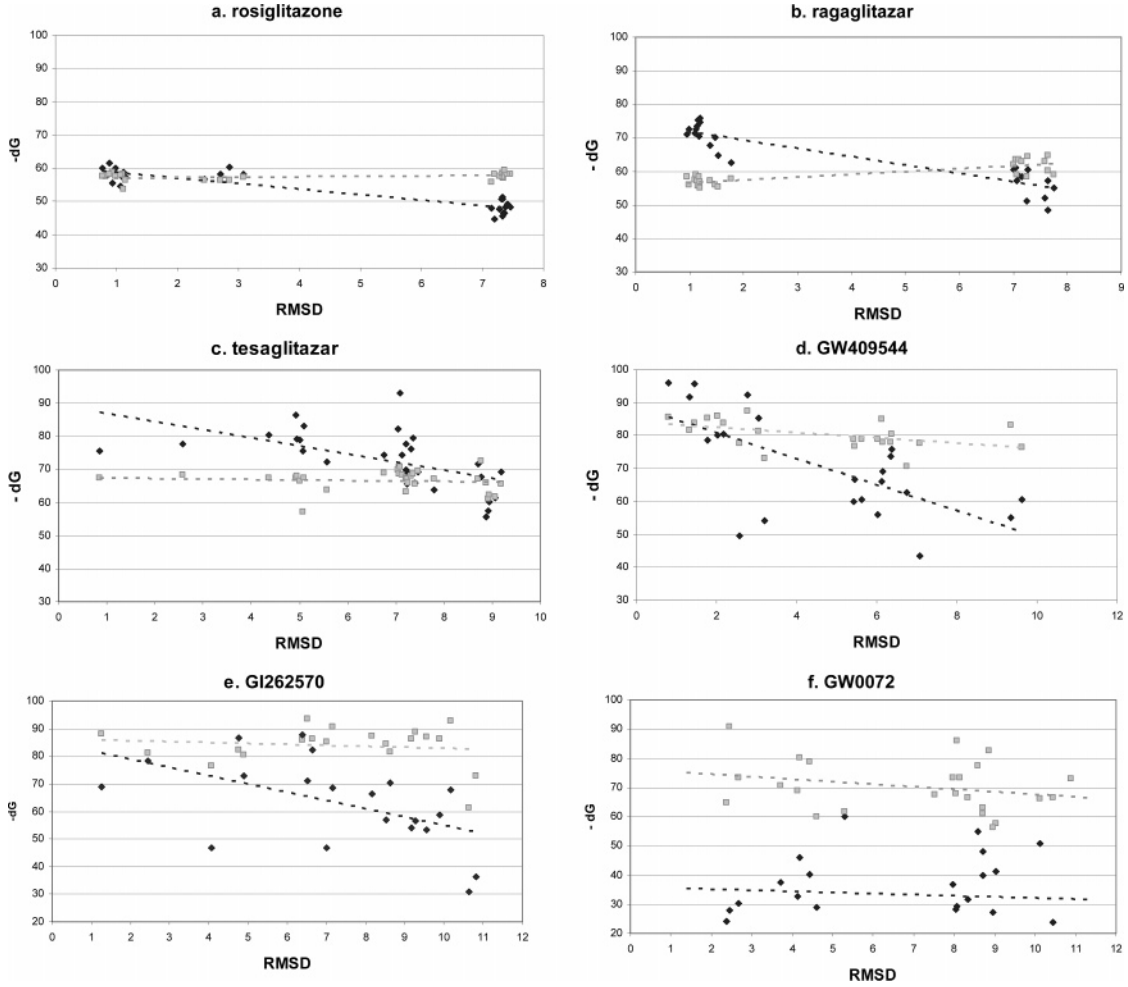

Figure 2. Discrimination of docked orientations using GOLD scoring (◆) as compared to CHARMM/ACE binding free energy (■): (a) rosiglitazone (**1**); (b) ragaglitazar (**2**); (c) tesaglitazar (AZ242) (**3**); (d) GW409544 (**4**); (e) GI262570 (**5**); and (f) GW0072 (**6**). Only clustered solutions are shown.

For comparison with the GOLD score, we use the negative of the binding free energy, i.e., $-\Delta G_{\mathrm{CHARMM}}$, as the CHARMM score.

Results

Docking of Known PPARγ Agonists. As described in the Materials and Methods, we generated 50 docked conformations for each of the six known PPAR-γ agonists shown in Figure 1. Figure 2 shows the correlations between the calculated GOLD scores ($-\Delta G_{\mathrm{GOLD}}$) and the ligand RMSDs from the native structure. The 50 conformations were subsequently refined and scored using the CHARMM/ACE potential. Figure 2 also shows the $-\Delta G_{\mathrm{CHARMM}}$ values obtained in these latter calculations. GOLD generates conformations with RMSD values from 1 to 12 Å. Because the correlation between the RMSD values and the scores is rather weak, the latter are generally unable to identify reliably the near-native conformations among the docked structures (see Discussion).

Figure 2a shows the docking results for rosiglitazone (**1**), the best-known PPAR agonist and insulin-sensitizing drug used to treat type II diabetes (*14*). The conformations from the 50 docking runs form three well-defined clusters, which deviate 1, 2.9, and 7.4 Å, respectively, from the native orientation. The cluster at 7.4 Å has a substantially lower average GOLD score than the other two and can be eliminated. However, the GOLD score cannot discriminate between the two clusters that are at 1 and 2.9 Å RMSD, respectively, from the native orientation. When used for discrimination, the CHARMM/ACE score performs even worse. As also shown in Figure 2a, the CHARMM/ACE values are essentially identical for all three clusters, including the one 7.4 Å from the native pose. However, as we will discuss, this invariance of the CHARMM/ACE scores provides some advantage when trying to predict the relative binding affinities of several compounds.

The best docking results were obtained for ragaglitazar **2**, a dual agonist, which activates both PPARα and PPARγ. As shown in Figure 2b, the docked poses from the 50 docking runs form two large clusters, the first cluster representing the most accurate docked orientations within 1 Å RMSD from the crystal structure. The GOLD score successfully discriminated between the two distinct types of docked complexes at 1 and 7.5 Å RMSD, whereas the CHARMM/ACE values did not.

For both compounds **1** and **2**, which have, respectively, seven and nine rotatable bonds, GOLD successfully populated the ligand space around the native (crystal structure) pose. As shown in Figure 2c−f, fewer docked orientations were observed within 2 Å RMSD from the native pose for compounds having 11 or more rotatable bonds (i.e., compounds **3**−**6**). In particular, the partial agonist GW0072 **6** has 18 rotatable bonds, which influenced the GOLD docking runs, resulting in five clusters. Each cluster has only a limited number of conformations; hence, the different clusters are difficult to distinguish (Figure 2f). Similar results have been reported regarding decreased accuracy in docking for ligand molecules with high numbers of rotatable bonds for a variety of docking software packages (*34*).

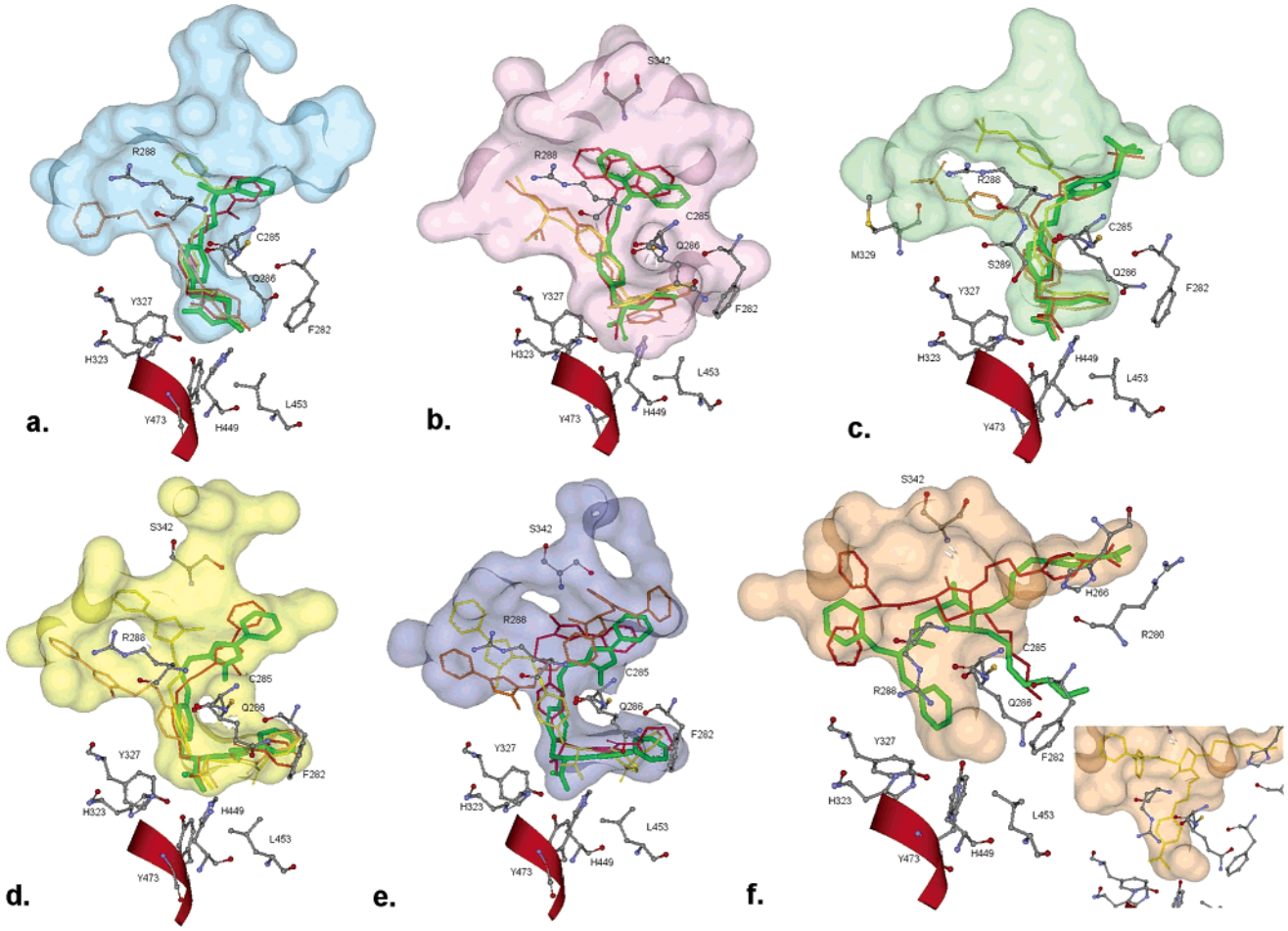

Figure 3. Docked orientations of agonists superimposed on crystal structure orientations (green) shown in the cavity of the PPAR-γ LBD. (a) Rosiglitazone, (b) ragaglitazar, (c) tesaglitazar (AZ242), (d) farglitazar (GW409544), (e) GI262570, and (f) GW0072 (partial agonist). For clarity, the inset in panel f separately shows the positional orientation of a cluster where the aromatic −COOH interacts with AF-2 residues in a way similar to ligands shown in panels b−e. Selected orientations are shown in red, yellow, and orange, with increasing RMSD deviation from the orientation in the X-ray structure. The amino acid side chains shown at the bottom of each image belong to the AF-2 activation domain (helix H12). The red ribbon indicates the path of the helical backbone of AF-2. The colored surfaces show the VDW surface of the binding cavity in each structure as determined by SPHGEN (*35*). Images were created with ViewerLite 5.0 (Accelrys Inc., 2002).

Geometry of Docked Conformations. Figure 3 shows the positions of docked ligands and interacting residues for the six PPARγ agonists given in Figure 1. The X-ray structure orientation of each ligand is given in green. Representative docked orientations are also shown, in red, yellow, and orange from each of the three clusters with the highest GOLD score. For clarity, we display only three clusters even if more than three were found. Figure 3 also shows residues H323, H449, Y473, and S289 of the transcriptional activation function 2 (AF-2) region, as well as helix 12 (H12). Agonists interact with these residues and stabilize H12 in an active conformation (*26*−*29*, *32*, *33*).

The docked poses of rosiglitazone **1** form three clusters (Figure 2a). In all three clusters, the thiazolidinedione (TZD) group interacts with the AF-2 region (Figure 3a), but the conformations differ from each other in placement of the pyridine ring-containing tail. The first two clusters, shown in red and yellow in Figure 3a, are significantly closer to the native pose than the third one shown in orange, in which the pyridine group forms a hydrogen bond with R288 at the far side of the pocket (shown on the left in Figure 3a). This variation in tail position may arise from the removal of bound water molecules that surround the pyridine ring in the crystal structure.

The second ligand, ragaglitazar, contains a carboxylic acid group, found in most PPAR agonists, rather than the heteroatom headgroup of the TZDs (*20*, *21*). This group interacts with AF-2 region residues H323, H449, Y473, and S289, i.e., the same residues that interact with the TZD group of rosiglitazone. Figure 3b shows a representative of this cluster in red, superimposed on the X-ray orientation of the ligand shown in green. The second cluster, at around 7.5 Å RMSD from the crystal structure, is actually formed by two subclusters, shown in yellow and orange in Figure 3b. In both subclusters, the ligand is oriented oppositely to the X-ray structure, with the −COOH group forming hydrogen bonds with R288 instead of the AF-2 domain residues.

In the case of AZ242 **3**, also called tesaglitazar, the position of the methylsulfonyl group differed from the crystal structure orientation in the majority of the docked structures, although the −COOH group was placed correctly for all three of the displayed clusters (Figures 2c and 3c). This variability could be attributed to the removal of water molecules in proximity to the sulfonyl group in the crystal structure (*22*). For GW409544 **4**, all three clusters interact with the AF-2 domain residues (Figure 3d), whereas for GI262570 **5** one cluster (orange) does not resemble the crystal structure in this regard (Figure 3e). For GW0072 **6**, the docked orientation, shown in red in Figure 3f, is the one closest to the crystal structure, but both phenyl rings are misplaced.

According to our results, the GOLD algorithm finds ligand orientations close to the crystal structure when docking known PPARγ agonists. These orientations were in highly populated clusters, which were subject to a certain level of positional variation, giving rise to some level of uncertainty. An increasing number of ligand rotatable bonds increased this variation, thereby reducing the number of near-native conformations generated in the 50 docking runs. The GOLD score generally identified the near-native poses of the ligands with limited degrees of rotational freedom but lost this ability as the number of rotatable bonds increased and thus the number of near-native poses decreased.

Docking of Phthalate Monoesters. After validating and assessing the limitations of GOLD docking results in the PPAR system, we applied the same methodology to the sets of *ortho*-phthalate monoesters shown in Table 1 and studied earlier (*7*, *9*). Docking calculations were carried out using the A chains in two PPARγ LBD structures, 2prgA and 4prgA, that substantially differ from each other in terms of the placement of key side chains, and thereby represent the uncertainty in the protein structure.

Figure 4 shows the correlations between EC_{50} and both GOLD and CHARMM scores for the *ortho*-phthalate monoesters in Table 1. According to these results, the GOLD scores weakly correlate with the experimental EC_{50} data for trans-activation for both receptor structures (Figure 4b,d). R^2 values were 0.31 and 0.44 for docking to 2prgA and 4prgA, respectively. Rosiglitazone **1**, activating phthalates, and nonactivating phthalates were clearly distinguishable from each other, except for compounds **13** and **14** in Table 1, for which the GOLD scores were out of the range of the others. The docked poses were subjected to a 100 step minimization using the CHARMM/ACE potential, and the CHARMM score, $-\Delta G_{CHARMM}$, was calculated as described in the Materials and Methods. As shown in Figure 4a,c, the measured log EC_{50} values correlate very well with the calculated free energies of the lowest free energy docked conformations, resulting in R^2 values of 0.82 and 0.69 for docking to 2prgA and 4prgA, respectively. Notice that the two outliers, compounds **13** and **14**, behave substantially better after the CHARMM minimization, although the scores are still artifactually high for phthalate **13**. This compound is fairly hydrophobic and scores above the mean GOLD score for the activating phthalates for both protein structures 2prgA and 4prgA. The other outlier, compound **14**, was penalized for steric interaction between its *tert*-butyl and methyl groups, but these interactions were more favorable after the CHARMM minimization.

Geometry of the Docked Phthalates. In addition to the compounds of the TZD family, PPARs are activated by acidic lipophilic ligands, such as fatty acids (*14*), which interact with the AF-2 domain through a number of hydrogen bonds, besides having close lipophilic interactions with the rest of the pocket. We expected a similar interaction to be present for the phthalates studied, where the phthalic acid carboxyl group would be hydrogen-bonded primarily to AF-2 domain residues. We therefore clustered the docked orientations of phthalates based on RMSD and compared the final positioning of major clusters of activating phthalates with the nonactivating phthalates, which were smaller in size.

Two major clusters were observed for orientations of activating phthalates docked to 2prgA. In cluster I orientations, the phthalic acid ring was situated in the vicinity of the AF-2 domain, making hydrogen bonds with H323 and nearby residues. This particular interaction resembles the crystal structure interactions of agonist compounds such as TZDs, which are known to facilitate trans-activation through stabilizing the activating conformation of H12, and it was absent in docked poses of nonactivating phthalates **19**−**21** (Table 1). Docked solutions for cluster II occurred in the center of the pocket, where the phthalic acid carboxyl group was hydrogen bonded to R288 rather than to the residues on H12.

Although docked orientations in cluster I were observed for a majority of the activating phthalates, cluster II dominated among these compounds. For phthalates with long alkyl ester chains, these chains fell into two distinct poses among the cluster II orientations: They either penetrated the AF-2 cavity of the pocket (Figure 5a, shown in pink) or extended toward the opposite side of the pocket around L353 and M360, filling in the cavity occupied by the tail of TZD type ligands (not shown). A majority of the phthalates with bulky ester groups, e.g., **13**−**16** and **18**, were docked in a tight cluster resembling the first subgroup of cluster II, partly penetrating the AF-2 site and making close hydrophobic contacts with the pocket. By contrast, the nonactivating phthalates lacked the lipophilic interactions described above; yet, they were positioned at the center of the pocket, making hydrogen bonds with R288 but not interacting with AF-2 domain residues.

Comparison of Bound Conformations of Agonists and Phthalates. To compare the phthalate poses to those of agonists, we note that the partial agonist GW0072 **6** and the strong agonist rosiglitazone **1** differ significantly in the way that they interact with the PPARγ LBD pocket, as well as in the characteristics of their trans-activational responses (*25*, *33*). The crystal structure of PPARγ bound to GW0072 **6** (4prg) exhibits a number of structural differences from the rosiglitazone-bound structure in terms of placement of critical residue side chains, besides the lack of direct interaction with the AF-2 domain (*33*). As part of these ligand-specific, induced-fit perturbations, R288 undergoes a major rearrangement and is positioned closer to Q286 in the partial agonist-bound structure, facing toward the AF-2 domain residues, as opposed to being in proximity to E295 (see Figure 5a,b). Therefore, R288 is no longer available for hydrogen bonding in the central pocket, as also seen from our docking results, since cluster II orientations no longer dominate the solution cluster but are replaced by three separate clusters shown in green, yellow, and turquoise in Figure 5b,d. The various poses in these three clusters all make hydrogen bonds to the backbone N atoms of distal pocket residues such as L22, K59, and S342. In the X-ray structure, the latter residue also forms a hydrogen bond with the carbonyl-oxygen atom of the central ring of partial agonist **6**. Only the subclusters shown in yellow in Figure 5b,d interact directly with the AF-2 domain. In this conformation, the carboxyl group hydrogen bonds to S342 and the alkyl tail partly penetrates the AF-2 region. Cluster I orientations, on the other hand, are hydrogen-bonded to H323 and H449, similar to strong agonists, as well as to R288, which is not the case in 2prg-docked poses (shown in red in Figure 5b,d).

Docking of Phthalate Monoesters from the ACD. We finally applied the above computational methods to investigate a broad set of phthalates from the ACD for possible binding to PPARγ. As described in the Materials and Methods, we extracted 73 mono-*ortho*-phthalates from among the 512 compounds bearing a phthalate moiety and applied the methodology described above to predict high-affinity PPARγ binding mono-*ortho*-phthalates. Thirteen of the 73 compounds have already been characterized experimentally with respect to PPARγ trans-activation (*7*, *9*). All of the four phthalate

Table 1. Transactivation of Phthalates (9)

No	Compound Name	Structure	EC_{50} (μM)	GOLD score	CHARMM - ΔG (kcal/mol)
7	mono-1-methyl-heptylphthalate(MHP)	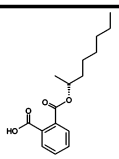	15	51.6	52.83
8	mono-1-methyl-hexylphthalate	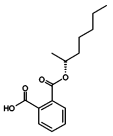	20	50.42	47.84
9	mono-2,2-dimethyl-1ethylpropylphthalate	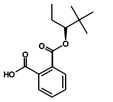	30	40.97	43.8
10	mono-2-ethyl-hexylphthalate (MEHP)	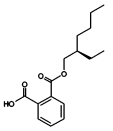	30	44.76	50.81
11	mono-benzylphthalate	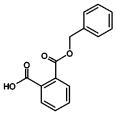	100	50.39	43.88
12	mono-2-(methacryloyloxy) ethylphthalate (MCE)	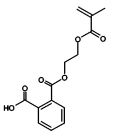	120	50.01	44.99
13	mono-(3chlorophenyl) phenylmethylphthalate	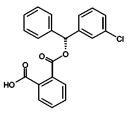	130	65.64	52.04
14	mono-2,2-dimethyl-1-isopropylpropylphthalate	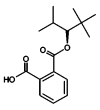	200	26.68	45.62
15	mono-1-tert-butyl-3-methylbutylphthalate	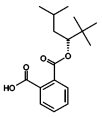	250	50.92	40.36
16	mono-1-methyl-2-norbonylphthalate	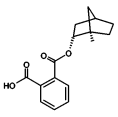	400	49.45	41.87
17	mono-1,2-dimethylpropylphthalate	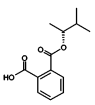	600	42.44	38.54
18	mono-alpha-ethyl-alpha-methylbenzylphtahalate	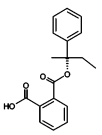	750	47.71	45.27
19	mono-methylphthalate		-	38.46	29.68
20	mono-ethylphthalate	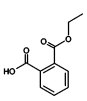	-	39.18	32.86
21	phthalic acid di-methyl-ester		-	37.49	33.58

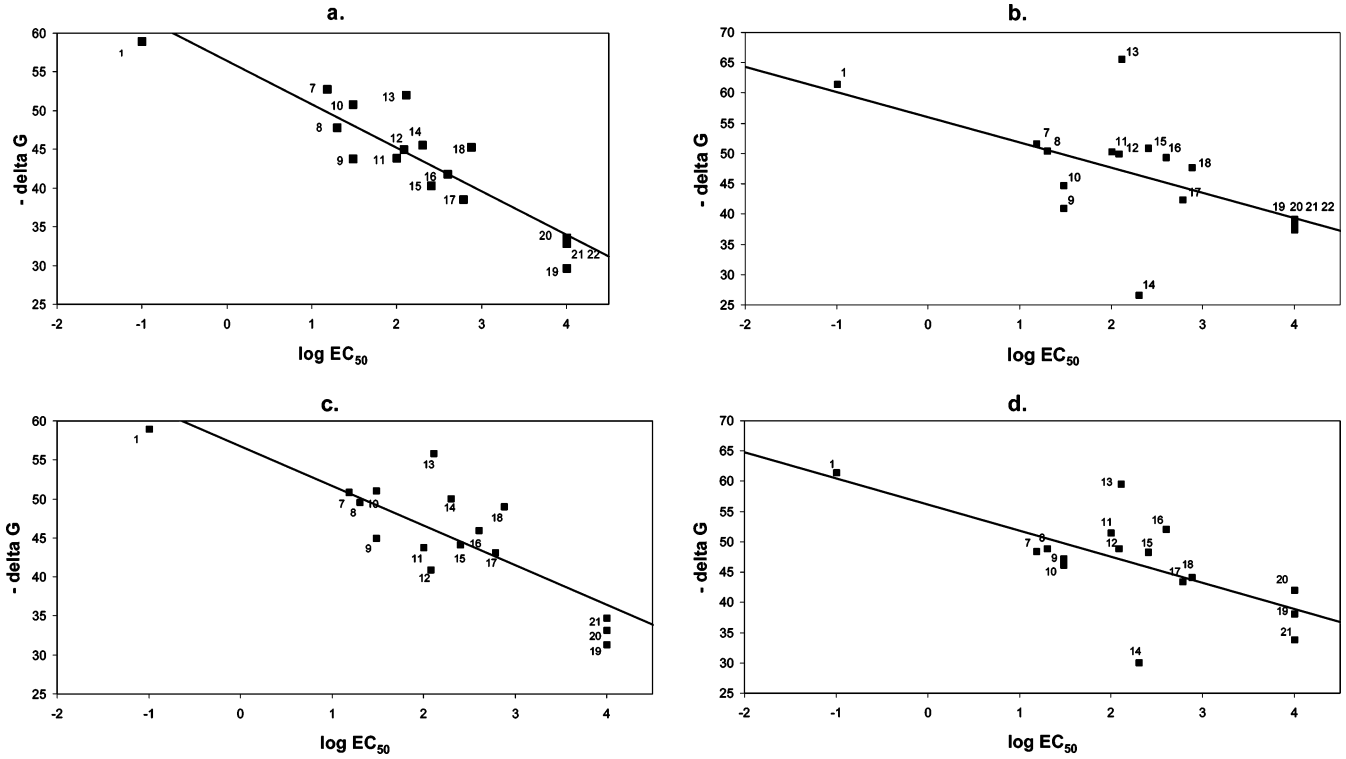

Figure 4. Correlation between EC_{50} and docking scores for the *ortho*-phthalate monoesters in Table 1. CHARMM/ACE scores are compared to GOLD scores for dockings to 2prgA and 4prgA. (a) CHARMM/ACE scores for 2prgA, $R^2 = 0.82$; (b) GOLD scores for 2prgA, $R^2 = 0.31$; (c) CHARMM/ACE scores for 4prgA, $R^2 = 0.69$; and (d) GOLD scores for 4prgA, $R^2 = 0.44$.

compounds with EC_{50} values <100 μM ranked within the top 35 hits with CHARMM scores greater than 50 kcal/mol, except for compound **15**, which was not included in the ACD. Table 2 lists the 20 monophthalates that were predicted to bind with the highest affinity, sorted by the CHARMM score, $-\Delta G_{C\text{-}HARMM}$. Notice that Table 2 excludes the phthalates listed in Table 1 and studied by Lampen (*9*) that were already discussed. Structures for nine of the high affinity monophthalates in Table 2 are shown in Figure 6.

Geometry of Predicted Activating Phthalates. The docked orientations of the top-scoring phthalates shown in Table 2 are similar to those shown in Figure 5 for activating phthalates. There are again two major clusters visible among docked orientations of the top five compounds from Table 2, in terms of placement of the phthalate functional group and ester chains. In cluster I solutions, residues in the vicinity of the AF-2 domain (H323, H449, Y327, Y473, and S289) again interact with the monophthalate ring and the −COOH functional group (shown in blue in Figure 7a−c for the phthalates **22**−**24**. Cluster II solutions are shown in yellow, pink, and green. Note that the solutions for **22** belong to both clusters I and II, since **22** has two monophthalate groups. The orientation shown in blue in Figure 7a was the dominant cluster, where one of the rings was placed in close proximity to the AF-2 region for 40 of the 50 docked solutions. Figure 7b,c shows cluster I (in blue) and several cluster II solutions for **23** and **24**. Compound **25** was found only in cluster II type orientations, with varying positions of the alkyl chain as shown in Figure 7d.

Discussion

We describe the application of molecular docking and free energy calculation methods to the problem of identifying monophthalates that are likely to act as PPARγ-activating environmental chemicals. Molecular docking simulations are widely used in structure-based drug design, where they provide useful information about key ligand−receptor interactions for known ligands as well as for putative ligands for which there may be little or no structural data. Nevertheless, they have limitations when it comes to reproducing the correct poses of bound ligands as found in crystal structures (docking) and the affinities associated with those poses (scoring). Moreover, docking and scoring are not completely independent since most procedures evaluate docked poses on the fly according to the main scoring scheme used by the algorithm.

To screen phthalates for binding to the PPARγ, we first focused on methodological issues. Test calculations applied to six known agonist-bound crystal structures showed that the GOLD docking algorithm was able to identify a binding mode for the ligands within 2 Å RMSD from the native crystal structure pose. However, the entire solution space for the docking typically consisted of several clusters of orientations. The presence of multiple docked orientations is largely a consequence of the shape of the interaction energy surface with multiple minima. The absence of some critical water molecules in the docking further complicates the phenomenon and introduces alternative binding modes. A portion of these binding modes can also be rationalized as secondary occupancy positions in the large and deep PPARγ binding pocket (*15*), which may or may not have physiological relevance.

The success rates in the docking calculations were largely determined by the ability to sample the region of near-native conformations which, in turn, was dependent on the size of the ligand. For ligands **1** and **2**, with seven and nine rotatable bonds, respectively, the algorithm generated many near-native poses, and the GOLD scoring function was able to discriminate these near-native clusters from other, non-native conformations. The fraction of near-native hits was lower for ligands **3**−**5** with higher numbers of rotatable bonds, and very few near-native solutions were found for the partial agonist **6** with 18 rotatable

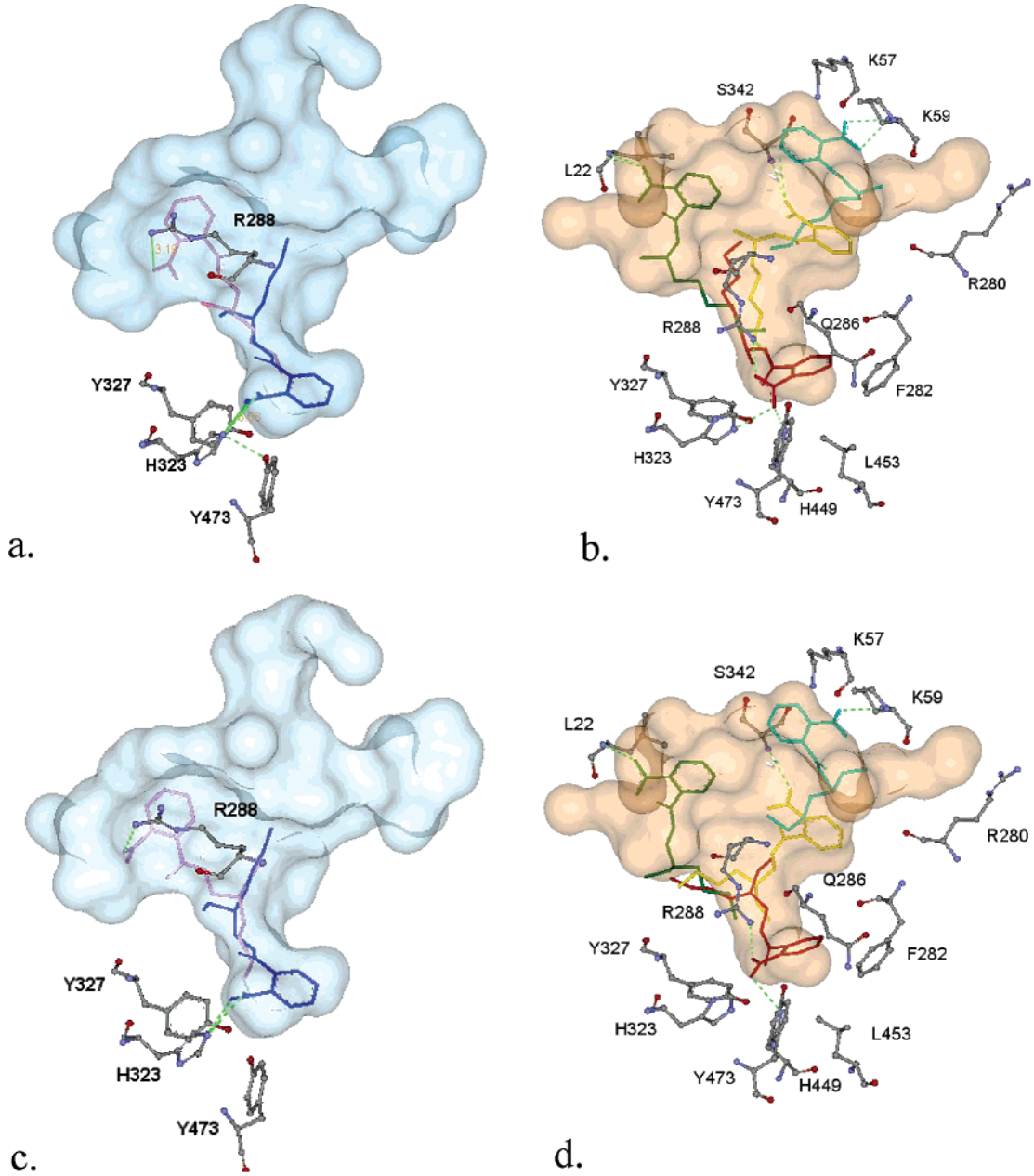

Figure 5. Docked orientations of mono-1-methylheptyl phthalate (MHP) and mono-2-ethylhexyl phthalate (MEHP) in two different PPAR-γ structures. (a) MHP in 2prgA. Clusters I and II are represented by the blue and pink poses, respectively. (b) MHP in 4prgA. The cluster I pose is shown in red; green, yellow, and turquoise are separate subclusters of cluster II. (c) MEHP in 2prgA; the color code is the same as in panel a. (d) MEHP in 4prgA; the color code is the same as in panel b. Dashed green lines indicate hydrogen bonds.

bonds. The GOLD score was also less successful in finding the fewer near-native poses among the generated structures. The difficulty of docking such "floppy" ligands has also been reported in the literature and explained by incomplete sampling of the conformational space (*34*). Further analysis revealed that results for compounds with many rotatable bonds can be somewhat improved by changing the parameters of the genetic algorithm in GOLD or simply increasing the number of docking runs (results not shown).

The main finding of this paper is the existence of the strong correlation between the EC_{50} values of the phthalate monoesters, determined by PPARγ activation experiments, and the CHARMM/ACE scores calculated for these compounds. This correlation is not perfect, given the fact that our computational model does not represent the in vivo system. Nevertheless, we were able to discriminate among potent, impotent, and nonactivating monophthalates using the CHARMM/ACE scoring function. The significance of this result is that it provides a relatively inexpensive approach to screening for compounds that are likely to activate PPARγ. In view of the inherent uncertainty of the computations, the candidate binders, once identified, need to be tested experimentally. Nevertheless, the number of molecules to be tested can be dramatically reduced making the computational approach highly cost-effective. Verification of monophthalates, potentially activating PPARγ (as well as exclusion of some candidates), should lead to a database of compounds that could enhance predictive capability and enable more effective regulatory actions.

In this paper, we performed the docking calculation using the GOLD method and tried to rank the poses with the GOLD scoring function. There are two reasons for restricting consideration to GOLD in docking. First, the performance of GOLD on a large test set of 305 complexes is very well-documented (*12*, *13*). Second, GOLD has been compared to essentially all

Table 2. *ortho*-Phthalate Monoesters with High Binding Affinity for PPAR-γ, Ranked by Decreasing CHARMM/ACE Score Defined as $-\Delta G_{CHARMM}$[a]

no.	compound name	GOLD score	CHARMM $-\Delta G$ (kcal/mol)
22	2-[([4-[(2-carboxybenzoyl)oxy]-1-methylpentyl]oxy)carbonyl]benzoic acid	55.98	69.02
23	phthalic acid mono-(biphenyl-4-yl-phenylmethyl) ester	71.92	66.86
24	10-undecenyl tetrachlorophthalate	54.29	65.88
25	2-octyl tetrachlorophthalate	53.7	60.58
26	3-nitro-phthalic acid 1-(1-methyl-2-phenylbutyl) ester	53.99	59.01
27	phthalic acid mono-(1-isopropyl-3-methyl-2-phenylbutyl) ester	37.47	57.38
28	3-nitro-phthalic acid 2-(1,2-diphenylpropyl) ester	56.28	57.30
29	3-nitro-phthalic acid 1-(1,2-diphenylpropyl) ester	57.64	56.31
30	phthalic acid mono-(1-isopropyl-3-methyl-2-phenylbutyl) ester	34.61	55.96
31	3-nitro-phthalic acid 1-(1,2-diphenylpropyl) ester	58.85	55.53
32	phthalic acid mono-bicyclo(10.2.2)hexadeca-1(15),12(16),13-trien-6-yl ester	54.74	55.19
33	phthalic acid mono-bicyclo(9.2.2)pentadeca-1(14),11(15),12-trien-5-yl ester	55.25	55.01
34	hexyl 3-nitro-phthalate	50.98	54.54
35	phthalic acid mono-(1-ethyl-2-phenylbutyl) ester	48.48	54.25
36	phthalic acid mono-bicyclo(9.2.2)pentadeca-1(14),11(15),12-trien-6-yl ester	49.19	54.13
37	3-nitro-phthalic acid 2-(3-methyl-2-phenylbutyl) ester	51.61	54.03
38	hexyl tetrachlorophthalate	54.02	53.81
39	phthalic acid mono-(1,2-diphenylpropyl) ester	55.17	53.26
40	2-methylpentyl tetrachlorophthalate	51.17	53.20
41	DL-mono-1-cyclohexyl-3-methylbutyl phthalate	49.11	52.95

[a] Compounds are named according to the usage in the ACD.

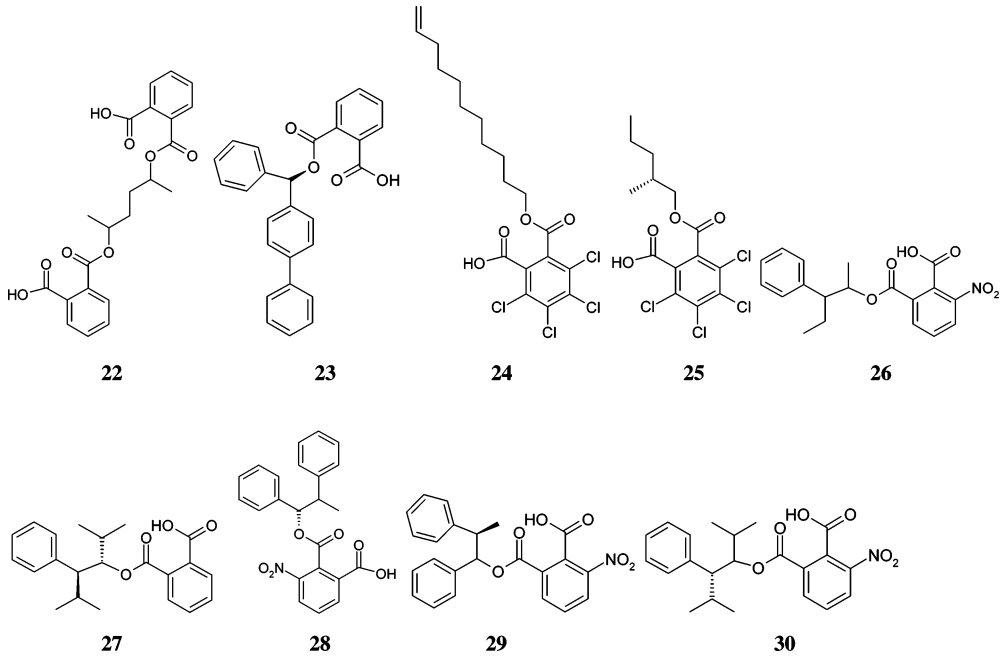

Figure 6. Structures of the top nine docked *ortho*-phthalate-monoesters selected from the ACD by computational docking to the 2prgA structure ranked by decreasing $-\Delta G$.

major docking programs currently in use, and it was found to be highly competitive (*38*−*41*). However, it was reported that docking scores and experimental binding affinities were poorly correlated (*14*, *42*−*44*), achieving R^2 values just over 0.5 (*14*, *42*). To improve results, we used a consensus scoring technique (*44*−*46*). The approach involves obtaining the output list of dockings with some search engine and primary score function (the GOLD algorithm and the GOLD score in this paper) and then rescoring the final list with a secondary score function (i.e., CHARMM/ACE here). While we have found GOLD scores superior in pose discrimination, the CHARMM/ACE values generally yield better correlation with the observed trans-activation. Indeed, in view of the low R^2 values reported in the literature (*14*, *42*), the correlation between the calculated energies and the logarithm of experimentally determined EC_{50} values is very strong, with R^2 values of 0.69 and 0.82, depending on the structure used. We need to emphasize that the calculation of the CHARMM/ACE energies requires minimization of the structure, and because it is computationally expensive, it cannot be used in high-throughput screening applications. However, with increasing computing power, the use of CHARMM-based methods becomes more feasible. It is particularly important that improved modeling of the receptor−ligand complex generally does not affect the results obtained by traditional scoring functions, but it can improve the accuracy of CHARMM energy calculations (*14*).

We emphasize that the CHARMM/ACE score generally predicts binding affinity and that affinity does not necessarily correlate with PPARγ trans-activation. For example, the partial agonist GW0072 **6** binds to PPARγ with higher affinity than rosiglitazone **1** does; yet, the transactivation of PPARγ by GW0072 is only 20−30% of its transactivation by rosiglitazone. The good correlation between the affinity and the level of PPARγ trans-activation, observed for phthalate monoesters, is

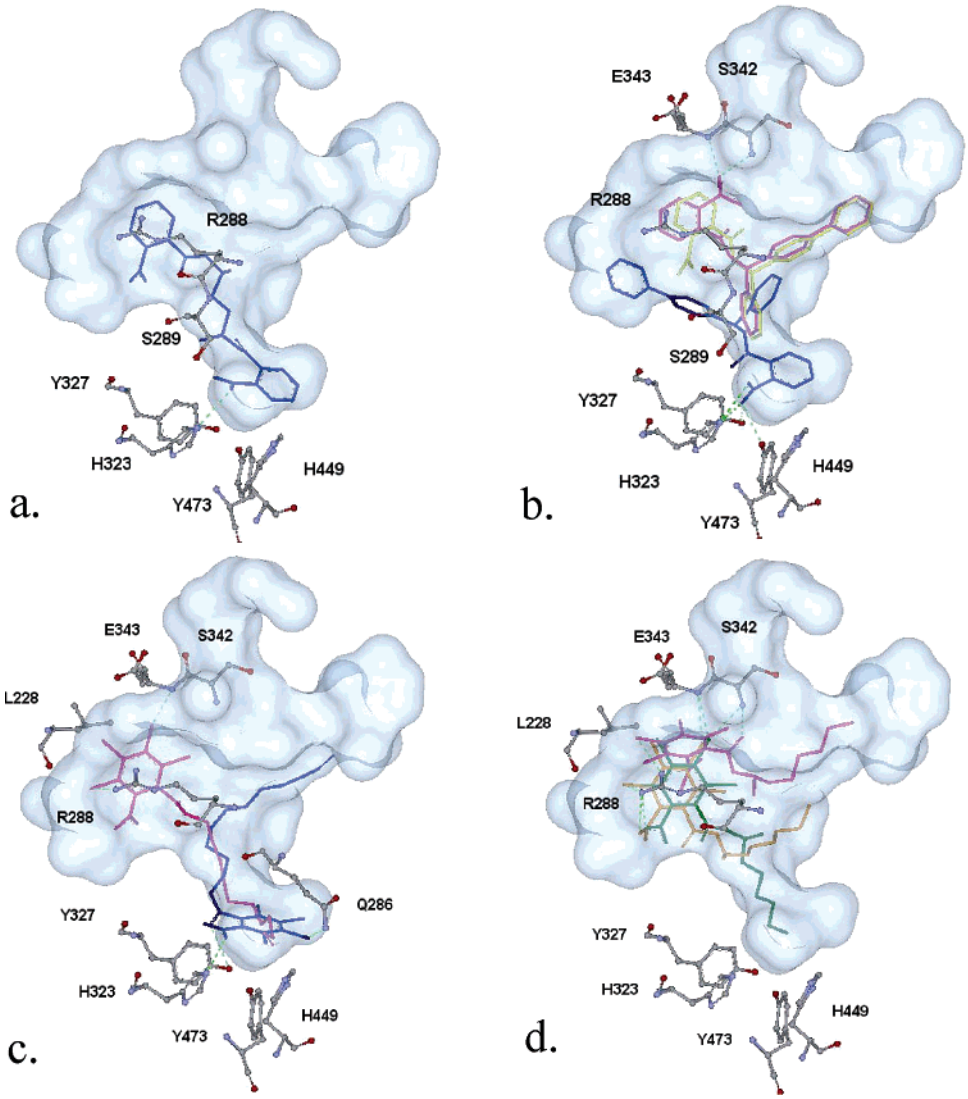

Figure 7. Docked orientations of top ranking *ortho*-phthalate-monoesters. (a) Compound **22**, (b) **23**, (c) **24**, and (d) **25**. Cluster I orientations are shown in blue, and cluster II orientations are in yellow, orange, and green. Dashed green lines indicate hydrogen bonds.

most likely due to the fact that we restrict consideration to compounds within a homologous family. A similar correlation may exist within other classes of homologous chemicals, but establishing the correlation requires further investigation for each class.

Although the method described in this paper does not necessarily predict PPARγ activation for an arbitrary compound, we have identified a useful algorithm for predicting the affinity of binding to PPARγ. The physically based CHARMM/ACE potential, in conjunction with a continuum electrostatic model of solvation, was shown to provide reasonable estimates of the relative binding free energies (*36*, *37*). In particular, it was somewhat unexpected to find that the CHARMM/ACE energy is much less dependent on the conformation than the GOLD score. Thus, minimization and rescoring using the CHARMM/ACE potential do not help to select near-native conformations but make the screening for activating phthalates essentially invariant to conformational differences on the docked poses and on the receptor structure. In fact, calculations on two considerably different PPARγ structures, 2prg and 4prg, yielded very similar results. Because accounting for protein flexibility in docking calculations is difficult and rarely attempted, the invariance of the calculated binding free energies is potentially very useful.

As described in this paper, the algorithm based on the combined use of the programs GOLD and CHARMM, both available either commercially or from academic sources, provides a general and robust method of estimating relative binding free energies for any family of compounds. Future studies may include experimental validation of the present predictions regarding phthalate monoesters and screening the ACD for novel classes of PPARγ binding molecules. However, even moderately strong correlations between docking scores and experimental binding affinities can be expected only within homologous classes of compounds but not necessarily for compounds from substantially different classes (*14*, *40*−*43*). Thus, although it is likely that screening the ACD for nonphthalate PPARγ binding molecules would yield apparent hits, the uncertainty of scoring makes the value of such analysis questionable.

Acknowledgment. This investigation was supported by Grant P42 ES07381 from the National Institute of Environmental Health Sciences and Grant GM064700 from the National Institute of General Medical Sciences.

References

(1) Cadogan, D. F. (1999) Plasticizers. In *Kirk-Othmer Concise Encyclopedia of Chemical Technology* (Kroschwitz, J. I., Ed.) pp 1577−1582, Wiley, New York.

(2) Blount, B. C., Silva, M. J., Caudill, S. P., Needham, L. L., Pirkle, J. L., Sampson, E. J., Lucier, G. W., Jackson, R. J., and Brock, J. W. (2000) Levels of seven urinary phthalate metabolites in a human reference population. *Environ. Health Perspect. 108*, 979−982.

(3) Silva, M. J., Barr, D. B., Reidy, J. A., Malek, N. A., Hodge, C. C., Caudill, S. P., Brock, J. W., Needham, L. L., and Calafat, A. M. (2004) Urinary levels of seven phthalate metabolites in the U.S. population from the National Health and Nutrition Examination Survey (NHANES) 1999−2000. *Environ. Health Perspect. 112*, 331−338.

(4) Tickner, J. A., Schettler, T., Guidotti, T., McCally, M., and Rossi, M. (2001) Health risks posed by use of di-2-ethylhexyl phthalate (DEHP) in PVC medical devices: a critical review. *Am. J. Ind. Med. 39*, 100−111.

(5) David, R. M., Moore, M. R., Cifone, M. A., Finney, D. C., and Guest, D. (1999) Chronic peroxisome proliferation and hepatomegaly associated with the hepatocellular tumorigenesis of di(2-ethylhexyl)-phthalate and the effects of recovery. *Toxicol. Sci. 50*, 195−205.

(6) Lovekamp-Swan, T., and Davis, B. J. (2003) Mechanisms of phthalate ester toxicity in the female reproductive system. *Environ. Health Perspect. 111*, 139−145.

(7) Hurst, C. H., and Waxman, D. J. (2003) Activation of PPARα and PPARγ by environmental phthalate monoesters. *Toxicol. Sci. 74*, 297−308.

(8) Swan, S. H., Main, K. M., Liu, F., Stewart, S. L., Kruse, R. L., Calafat, A. M., Mao, C. S., Redmon, J. B., Ternand, C. L., Sullivan, S., and Teague, J. L. (2005) Study for Future Families Research (2005). Decrease in anogenital distance among male infants with prenatal phthalate exposure. *Environ. Health Perspect. 113* (8), 1056−1061.

(9) Lampen, A., Zimnik, S., and Nau, H. (2003). Teratogenic phthalate esters and metabolites activate the nuclear receptors PPARs and induce differentiation of F9 cells. *Toxicol. Appl. Pharmacol. 188*, 14−23.

(10) Jones, G., Willett, P., and Glen, R. C. (1995). Molecular recognition of receptor sites using a genetic algorithm with a description of desolvation. *J. Mol. Biol. 245*, 43−53.

(11) Jones, G., Willett, P., Glen, R. C., Leach, A. R., and Taylor, R. (1997). Development and validation of a genetic algorithm for flexible docking. *J. Mol. Biol. 267*, 727−748.

(12) Nissink, J. W. M., Murray, C., Hartshorn, M., Verdonk, M. L., Cole, J. C., and Taylor, R. (2002) A new test set for validating predictions of protein−ligand interaction. *Proteins 49*, 457−471.

(13) Verdonk, M. L., Cole, J. C., Hartshorn, M. J., Murray, C. W., and Taylor, R. D. (2003) Improved protein−ligand docking using GOLD. *Proteins 52*, 609−623.

(14) Ferrara, P., Gohlke, H., Price, D. J., Klebe, G., and Brooks, C. L., 3rd (2004) Assessing scoring functions for protein−ligand interactions. *J. Med. Chem. 47*, 3032−3047.

(15) Nolte, R. T., Wisely, G. B., Westin, S., Cobb, J. E., Lambert, M. H., Kurokawa, R., Rosenfeld, M. G., Willson, T. M., Glass, C. K., and Milburn, M. V. (1998) Ligand binding and co-activator assembly of the peroxisome proliferators-activated receptor-γ. *Nature 395*, 137−144.

(16) Bernstein, F. C., Koetzle, T. F., Williams, G. J. B., Meyer, E. F., Jr., Brice, M. D., Rodgers, J. R., Kennard, O., Shimanouchi, T., and Tasumi, M. (1977) The Protein Data Bank: A computer-based archival file for macromolecular structures. *J. Mol. Biol. 112*, 535−542.

(17) Brooks, B. R., Bruccoleri, R. E., Olafson, B. D., States, D. J., Swaminathan, S., and Karplus, M. (1983) CHARMM: A program for macromolecular energy, minimization, and dynamics calculations. *J. Comput. Chem. 4*, 187−217.

(18) MacKerell, A. D., Jr., Brooks, B., Brooks, C. L., Nilsson, L., III, Roux, B., Won, Y., and Karplus, M. (1998) CHARMM: The energy function and its parametrization with an overview of the program. *Encycl. Comput. Chem. 1*, 271−277.

(19) Schaefer, M., and Karplus, M. A. (1996) A comprehensive analytical treatment of continuum electrostatics. *J. Phys. Chem. 100*, 1578−1599.

(20) Adams, A. D., Yuen, W., Hu, Z., Santini, C., Jones, A. B., MacNaul, K. L., Berger, J. P., Doebber, T. W., Moller, D. E. (2003) Amphipathic 3-Phenyl-7-propylbenzisoxazoles; human PPAR γ, δ and α agonists. *Bioorg. Med. Chem. Lett. 13*, 931−935.

(21) Sauerberg, P., Pettersson, I., Jeppesen, L., Bury, P. S., Mogensen, J. P., Wassermann, K., Brand, C. L., Sturis, J., Woldike, H. F., Fleckner, J., Andersen, A. S., Mortensen, S. B., Svensson, L. A., Rasmussen, H. B., Lehmann, S. V., Polivka, Z., Sindelar, K., Panajotova, V., Ynddal, L., and Wulff, E. M. (2002). Novel tricyclic-α-alkyloxyphenylpropionic acids: Dual PPAR α/γ agonists with hypolipidemic and antidiabetic activity. *J. Med. Chem. 45*, 789−804.

(22) Cronet, P., Petersen, J. F., Folmer, R., Blomberg, N., Sjoblom, K., Karlsson, U., Lindstedt, E. L., and Bamberg, K. (2001) Structure of the PPARα and -γ ligand binding domain in complex with AZ242; Ligand selectivity and agonist activation in the PPAR family. *Structure 9*, 699−706.

(23) Xu, H. E., Lambert, M. H., Montana, V. G., Plunket, K. D., Moore, L. B., Collins, J. L., Oplinger, J. A., Kliewer, S. A., Gampe, R. T., Jr., McKee, D. D., Moore, J. T., and Willson, T. M. (2001) Determinants of ligand binding selectivity between the peroxisome proliferator-activated receptors. *Proc. Natl. Acad. Sci. U.S.A. 98*, 13919−13924.

(24) Gampe, R. T., Montana, V. G., Lambert, M. H., Miller, A. B., Bledsoe, R. K., Milburn, M. V., Kliewer, S. A., Willson, T. M., and Xu, H. E. (2000) Asymmetry in the PPARγ/RXRα crystal structure reveals the molecular basis of heterodimerization among nuclear receptors. *Mol. Cell 5*, 545−555.

(25) Oberfield, J. L., Collins, J. L., Holmes, C. P., Goreham, D. M., Cooper, J. P., Cobb, J. E., Lenhard, J. M., Hull-Ryde, E. A., Mohr, C. P., Blanchard, S. G., Parks, D. J., Moore, L. B., Lehmann, J. M., Plunket, K., Miller, A. B., Milburn, M. V., Kliewer, S. A., and Willson, T. M. (1999) A peroxisome proliferators-activated receptor γ inhibits adipocyte differentiation. *Proc. Natl. Acad. Sci. U.S.A. 96*, 6102−6106.

(26) Berger, J., and Moller, D. E. (2002) The mechanism of action of PPARs. *Annu. Rev. Med. 53*, 409−435.

(27) Nettles, K. W., Sun, J., Radek, J. T., Sheng, S., Rodriguez, A. L., Katzenellenbogen, J. A., Katzenellenbogen, B. S., and Greene, G. L. (2004) Allosteric control of ligand selectivity between estrogen receptors α and β: Implications for other nuclear receptors. *Mol. Cell 13*, 317−327.

(28) Nagy, L., and Schwabe, J. W. R. (2004) Mechanism of the nuclear receptor molecular switch. *Trends Biochem. Sci. 29*, 317−324.

(29) Li, Y., Lambert, M. H., and Xu, H. E. (2003) Activation of nuclear receptors: A perspective from structural genomics. *Structure 11*, 741−746.

(30) Gasteiger, J., and Marsili, M. (1978) A new model for calculating atomic charges in molecules. *Tetrahedron Lett.* 3181−3184.

(31) Walters, P., and Stahl, M. *BABEL*, Department of Chemistry, University of Arizona.

(32) Pissios, P., Tzameli, I., Kushner, P., and Moore, D. D. (2000) Dynamic stabilization of nuclear receptor ligand binding domains by hormone or corepressor binding. *Mol. Cell 6*, 245−253.

(33) Sheu, S.-H., Kaya, T., Waxman D. J., and Vajda, S. (2005) Exploring the binding site structure of the PPAR-γ ligand binding domain by computational solvent mapping. *Biochemistry 44*, 1193−1209.

(34) Erickson, J. A., Jalaie, M., Robertson, D. H., Lewis, R. A., and Vieth, M. (2004) Lessons in molecular recognition: The effects of ligands and protein flexibility on molecular docking accuracy. *J. Med. Chem. 47*, 45−55.

(35) Connolly, M. L. (1983) Solvent-accessible surfaces of proteins and nucleic acids. *Science 221*, 709−713.

(36) Zoete, V., Michielin, O., and Karplus, M. (2003) Protein−ligand binding free energy estimation using molecular mechanics and continuum electrostatics. Application to HIV-1 protease inhibitors. *J. Comput.-Aided Mol. Des. 17*, 861−880.

(37) Zoete, V., Meuwly, M., and Karplus, M. (2005) Study of the insulin dimerization: Binding free energy calculations and per-residue free energy decomposition. *Proteins 61*, 79−93.

(38) Kellenberger, E., Rodrigo, J., Muller, P., and Rognan, D. (2004) Comparative evaluation of eight docking tools for docking and virtual screening accuracy. *Proteins 57*, 225−242.

(39) Kontoyianni, M., McClellan, L. M., and Sokol, G. S. (2004) Evaluation of docking performance: Comparative data on docking algorithms. *J. Med. Chem. 47*, 558−565.

(40) Perola, E., Walters, W. P., and Charifson, P. S. (2004) A detailed comparison of current docking and scoring methods on systems of pharmaceutical relevance. *Proteins 56*, 235−249.

(41) Cummings, M. D., DesJarlais, R. L., Gibbs, A. C., Mohan, V., and Jaeger, E. P. (2005) Comparison of automated docking programs as virtual screening tools. *J. Med. Chem. 48*, 962−976.

(42) Wang, R., Lu, Y., and Wang, S. (2003) Comparative evaluation of 11 scoring functions for molecular docking. *J. Med. Chem. 46*, 2287−2303.

(43) Wang, R., Lu, Y., Fang, X., and Wang, S. (2004) An extensive test of 14 scoring functions using the PDBbind refined set of 800 protein−ligand complexes. *J. Chem. Inf. Comput. Sci. 44*, 2114−2125.

(44) Mohan, V., Gibbs, A. C., Cummings, M. D., Jaeger, E. P., and DesJarlais, R. L. (2005) Docking: Successes and challenges. *Curr. Pharm. Des. 11*, 323−333.

(45) Charifson, P. S., Corkery, J. J., Murcko, M. A., and Walters, W. P. (1999) Consensus scoring: A method for obtaining improved hit rates from docking databases of three-dimensional structures into proteins. *J. Med. Chem. 42*, 5100−5109.

(46) Paul, N., and Rognan, D. (2002) ConsDock: A new program for the consensus analysis of protein−ligand interactions. *Proteins 47*, 521−533.